

QCD Thermodynamics at Finite Temperature and Finite Chemical Potential

NAJMUL HAQUE*

Theory Division, Saha Institute of Nuclear Physics, 1/AF Bidhannagar, Kolkata 700 064 India

(Received on 11 May 2014; Accepted on 9 September 2014)

We calculate thermodynamic functions *viz.* pressure, change in pressure due to chemical potential, quark number density of hot and dense nuclear matter at finite temperature and chemical potential using three-loop Hard Thermal Loop perturbation theory.

Key Words : Quantum Chromodynamics; Quark Gluon Plasma; Hard Thermal Loop Perturbation Theory; Temperature; Chemical Potential

Introduction

Quantum chromodynamics (QCD) exhibits a rich phase structure and describes the propagation and interaction of quarks and gluons which are the fundamental constituents of all hadronic matter. Based solely on the QCD Lagrangian it is possible to calculate the QCD partition function at finite temperature and finite chemical potential and it results in the so-called equation of state (EoS). The determination of the QCD EoS and other thermodynamical quantities are extremely important to the phenomenology of the hot and dense nuclear matter commonly known as quark-gluon plasma (QGP). At this time, the most reliable method to calculate the QCD thermodynamic functions at finite temperature and zero (small) chemical potential is lattice gauge theory (Borsanyi *et al.*, 2010, 2012a,b,c; Borsanyi 2013; Borsanyi *et al.*, 2009, 2012, 2013; Bernard *et al.*, 2005; Petreczky 2012). Importantly, lattice QCD can be used to probe the behaviour of QCD matter near the phase transition from the hadronic to the deconfined QGP phase. Near the phase transition temperature, the running coupling is large and non-perturbative methods like lattice QCD must be used. Finite temperature lattice QCD calculations are now quite stable; however, due to the sign problem, it is not straightforward to extend such calculations to finite baryon chemical potential. In practice, it is possible to obtain information about the behaviour of the thermodynamic functions at small baryon chemical potential

* Author for Correspondence : E-mail: najmul.haque@saha.ac.in

by making a Taylor expansion of the partition function around zero baryonic chemical potential and extrapolating the result. This requires the calculation of various order quark-number susceptibilities evaluated at zero chemical potential. Since extrapolations based on a finite number of term, Taylor coefficients can only be trusted at small value of chemical potential and it would be nice to have an alternative framework for calculating the finite temperature and chemical potential QCD thermodynamic potential and associated quantities. This is important in light of the ongoing beam energy scan at the Relativistic Heavy Ion Collider (RHIC) in Brookhaven National Laboratory (BNL) and at Large Hadron Collider (LHC) in European Organization for Nuclear Research (CERN) and also at the forthcoming experiments at the Facility for Antiproton and Ion Research (FAIR) in Gesellschaft für Schwerionenforschung (GSI). As an alternative to lattice QCD calculations, one natural option is to compute the thermodynamic potential using perturbation theory at finite temperature and at finite chemical potential. In principle, this should work since, at sufficiently high temperature, the value of the strong coupling constant is small; however, one does not know a priori how large the temperature should be for this method to give result which are close to reality within a good approximation.

Unfortunately, it turns out that a strict expansion in the coupling constant converges only for temperatures many orders of magnitude higher than those relevant for heavy-ion collision experiments. The source of the poor convergence comes from contributions from soft momenta, $p \sim gT$. This suggests that one needs a way of reorganising the perturbative series which treats the soft sector more carefully. As a result, a gauge-invariant reorganising called hard-thermal-loop perturbation theory (HTLpt) was developed by Braaten and Pisarski in Braaten *et al.*, (1990). HTL perturbation has been used to calculate thermodynamic functions and other thermodynamical quantities at one loop (Andersen *et al.*, 2000; Haque *et al.*, 2010, 2011a,b; Chakraborty *et al.*, 2002, 2003), at two loops (Andersen *et al.*, 2002; Haque *et al.*, 2013a,b) and at three loops at zero chemical potential (Su *et al.*, 2010); (Andersen *et al.*, 2009, 2010, 2011) as well as at finite chemical potential (Haque *et al.*, 2014b,a) within HTL perturbation theory.

Feynman Diagrams

Feynman diagrams that will contribute to the QCD thermodynamics potential up to three-loop in HTL approximation are listed below:

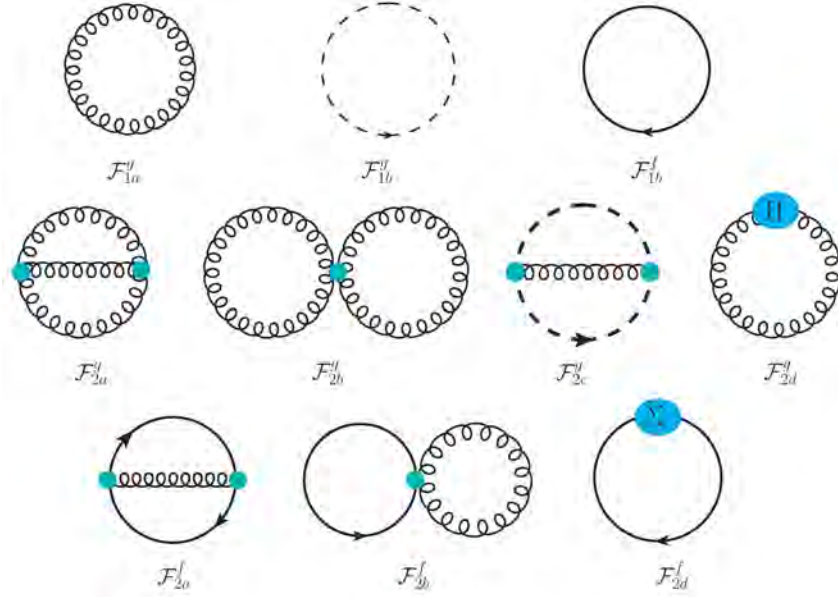


Fig. 1: One and two loop HTL Feynman diagrams contributing to the QCD thermodynamic potential

Thermodynamics Potential

The QCD thermodynamics potential up to three-loop HTL approximation including all the necessary counter term can be summarized as

$$\begin{aligned}
\frac{\Omega_{\text{NNLO}}}{\Omega_0} &= 1 + \frac{7 d_F}{4 d_A} \left(1 + \frac{120}{7} \hat{\mu}^2 + \frac{240}{7} \hat{\mu}^4 \right) - \frac{15}{4} \hat{m}_D^3 + \frac{c_A \alpha_s}{3\pi} \left[-\frac{15}{4} + \frac{45}{2} \hat{m}_D \right. \\
&- \frac{135}{2} \hat{m}_D^2 - \frac{495}{4} \left(\ln \frac{\hat{\Lambda}_g}{2} + \frac{5}{22} + \gamma_E \right) \hat{m}_D^3 \left. \right] + \left(\frac{c_A \alpha_s}{3\pi} \right)^2 \left[\frac{45}{4 \hat{m}_D} \right. \\
&- \frac{165}{8} \left(\ln \frac{\hat{\Lambda}_g}{2} - \frac{72}{11} \ln \hat{m}_D - \frac{84}{55} - \frac{6}{11} \gamma_E - \frac{74}{11} \frac{\zeta'(-1)}{\zeta(-1)} + \frac{19}{11} \frac{\zeta'(-3)}{\zeta(-3)} \right) \\
&+ \frac{1485}{4} \left(\ln \frac{\hat{\Lambda}_g}{2} - \frac{79}{44} + \gamma_E + \ln 2 - \frac{\pi^2}{11} \right) \hat{m}_D \left. \right] - \frac{s_F \alpha_s}{\pi} \left[\frac{5}{8} (1 + 12 \hat{\mu}^2) (5 + 12 \hat{\mu}^2) \right. \\
&- \frac{15}{2} (1 + 12 \hat{\mu}^2) \hat{m}_D - \frac{15}{2} \left(2 \ln \frac{\hat{\Lambda}}{2} - 1 - \aleph(z) \right) \hat{m}_D^3 + 90 \hat{m}_q^2 \hat{m}_D \left. \right] \\
&+ s_{2F} \left(\frac{\alpha_s}{\pi} \right)^2 \left[\frac{15}{64} \left\{ 35 - 32 (1 - 12 \hat{\mu}^2) \frac{\zeta'(-1)}{\zeta(-1)} + 472 \hat{\mu}^2 + 1328 \hat{\mu}^4 \right. \right. \\
&\left. \left. + 64 \left(-36 i \hat{\mu} \aleph(2, z) + 6(1 + 8 \hat{\mu}^2) \aleph(1, z) + 3i \hat{\mu} (1 + 4 \hat{\mu}^2) \aleph(0, z) \right) \right\} \right] \quad (1)
\end{aligned}$$

$$\begin{aligned}
& - \frac{45}{2} \hat{m}_D (1 + 12\hat{\mu}^2) \Big] + \left(\frac{s_F \alpha_s}{\pi} \right)^2 \left[\frac{5}{4\hat{m}_D} (1 + 12\hat{\mu}^2)^2 + 30 (1 + 12\hat{\mu}^2) \frac{\hat{m}_q^2}{\hat{m}_D} \right. \\
& + \frac{25}{12} \left\{ \left(1 + \frac{72}{5} \hat{\mu}^2 + \frac{144}{5} \hat{\mu}^4 \right) \ln \frac{\hat{\Lambda}}{2} + \frac{1}{20} (1 + 168\hat{\mu}^2 + 2064\hat{\mu}^4) + \frac{3}{5} (1 + 12\hat{\mu}^2)^2 \gamma_E \right. \\
& - \frac{8}{5} (1 + 12\hat{\mu}^2) \frac{\zeta'(-1)}{\zeta(-1)} - \frac{34}{25} \frac{\zeta'(-3)}{\zeta(-3)} - \frac{72}{5} \left[8\aleph(3, z) + 3\aleph(3, 2z) - 12\hat{\mu}^2 \aleph(1, 2z) \right. \\
& + \left. \left. 12i\hat{\mu} (\aleph(2, z) + \aleph(2, 2z)) - i\hat{\mu} (1 + 12\hat{\mu}^2) \aleph(0, z) - 2(1 + 8\hat{\mu}^2) \aleph(1, z) \right] \right\} \\
& - \frac{15}{2} \left\{ (1 + 12\hat{\mu}^2) \left(2 \ln \frac{\hat{\Lambda}}{2} - 1 - \aleph(z) \right) \right\} \hat{m}_D \Big] \\
& + \left(\frac{c_A \alpha_s}{3\pi} \right) \left(\frac{s_F \alpha_s}{\pi} \right) \left[\frac{15}{2\hat{m}_D} (1 + 12\hat{\mu}^2) - \frac{235}{16} \left\{ \left(1 + \frac{792}{47} \hat{\mu}^2 + \frac{1584}{47} \hat{\mu}^4 \right) \ln \frac{\hat{\Lambda}}{2} \right. \right. \\
& - \frac{144}{47} (1 + 12\hat{\mu}^2) \ln \hat{m}_D + \frac{319}{940} \left(1 + \frac{2040}{319} \hat{\mu}^2 + \frac{38640}{319} \hat{\mu}^4 \right) - \frac{24\gamma_E}{47} (1 + 12\hat{\mu}^2) \\
& - \frac{44}{47} \left(1 + \frac{156}{11} \hat{\mu}^2 \right) \frac{\zeta'(-1)}{\zeta(-1)} - \frac{268}{235} \frac{\zeta'(-3)}{\zeta(-3)} - \frac{72}{47} \left[4i\hat{\mu} \aleph(0, z) \right. \\
& + \left. \left. (5 - 92\hat{\mu}^2) \aleph(1, z) + 144i\hat{\mu} \aleph(2, z) + 52\aleph(3, z) \right] \right\} + 90 \frac{\hat{m}_q^2}{\hat{m}_D} \\
& + \frac{315}{4} \left\{ \left(1 + \frac{132}{7} \hat{\mu}^2 \right) \ln \frac{\hat{\Lambda}}{2} + \frac{11}{7} (1 + 12\hat{\mu}^2) \gamma_E + \frac{9}{14} \left(1 + \frac{132}{9} \hat{\mu}^2 \right) \right. \\
& + \left. \left. \frac{2}{7} \aleph(z) \right\} \hat{m}_D \Big], \tag{2}
\end{aligned}$$

where, with the standard normalization, the QCD Casimir numbers are $c_A = N_c$, $d_A = N_c^2 - 1$, $s_f = N_f/2$, $C_F = (N_c^2 - 1)/2N_c$, $s_{2f} = C_F s_f$. $\Omega_0 = -d_A \pi^2 T^4/45$, thermodynamic potential for free pure-gluon case. The sums over f and g include all quark flavors, $z_f = 1/2 - i\hat{\mu}_f$. The details about the functions $\aleph(z)$ and $\aleph(n, z)$ can be found in Haque *et al* (2014b,a). Here m_D and m_q are two parameters in HTL perturbation theory and we could identify these parameters as debye and thermal quark mass respectively. We have used here some scaled quantities as $\hat{m}_D = m_D/2\pi T$, $\hat{m}_q = m_q/2\pi T$, $\hat{\Lambda} = \Lambda/2\pi T$ and $\hat{\mu} = \mu/2\pi T$.

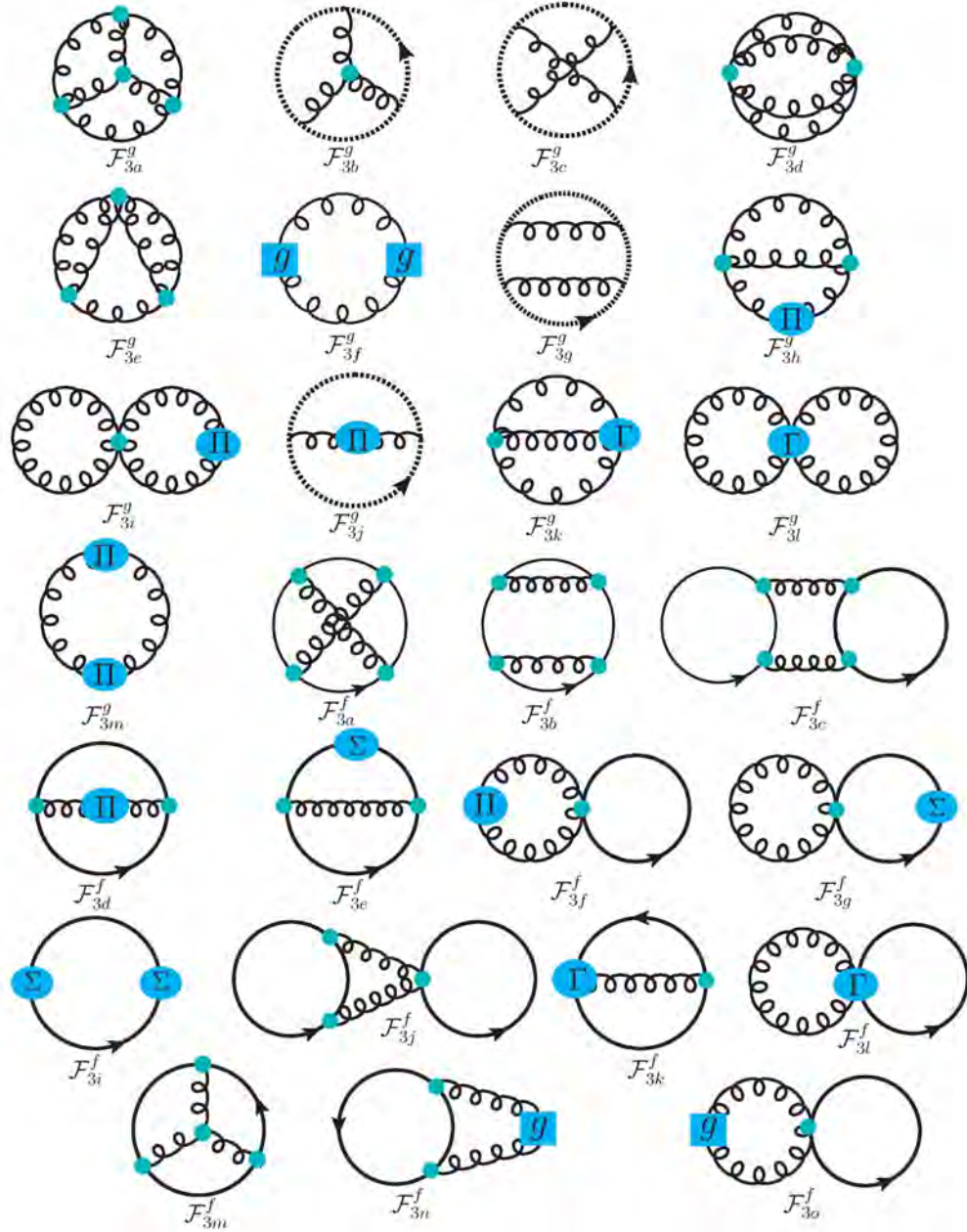


Fig. 2: Three loop HTL Feynman diagrams contributing to the QCD thermodynamic potential

Pressure

The QGP pressure can be obtained directly from the thermodynamic potential (2) as

$$\mathcal{P}(T, \Lambda, \Lambda_g, \mu) = -\Omega_{\text{NNLO}}(T, \Lambda, \Lambda_g, \mu), \quad (3)$$

In Fig. 3 we compare the scaled NNLO HTLpt pressure for $\mu_B = 0$ (A) and $\mu_B = 400\text{MeV}$ (B) with available recent lattice data where $\mu_B = \sum_{N_f} \mu_f$. It is worth to mention here that for numerical results, we use

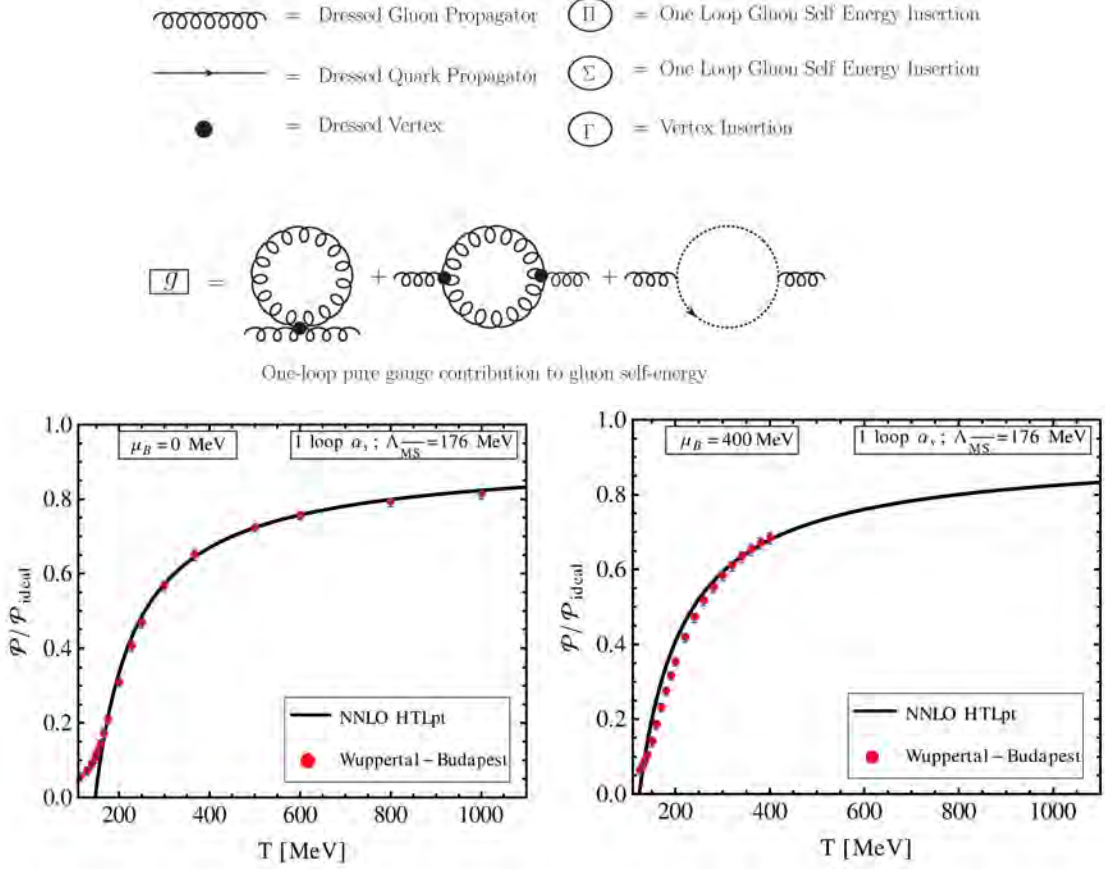


Fig. 3: Next-to-next leading order HTLpt QCD pressures at finite μ and zero μ scaled with free values for $\Lambda = 2\pi\sqrt{T^2 + \mu^2/\pi^2}$ and $\Lambda_g = 2\pi T$ with lattice data from Borsanyi *et al.* (2012c) with one-loop running coupling constant

$$\hat{m}_D^2 = \frac{\alpha_s}{3\pi} \left\{ c_A + s_F (1 + 12\hat{\mu}^2) + \frac{c_A^2 \alpha_s}{12\pi} \left(5 + 22\gamma_E + 22 \ln \frac{\hat{\Lambda}_g}{2} \right) + \frac{c_A s_F \alpha_s}{12\pi} \left((9 + 132\hat{\mu}^2) + 22 (1 + 12\hat{\mu}^2) \gamma_E + 2 (7 + 132\hat{\mu}^2) \ln \frac{\hat{\Lambda}}{2} + 4\aleph(z) \right) + \frac{s_F^2 \alpha_s}{3\pi} (1 + 12\hat{\mu}^2) \left(1 - 2 \ln \frac{\hat{\Lambda}}{2} + \aleph(z) \right) - \frac{3}{2} \frac{s_{2F} \alpha_s}{\pi} (1 + 12\hat{\mu}^2) \right\}, \quad (4)$$

$$\hat{m}_q^2 = \frac{C_F \alpha_s (1 + 4\hat{\mu}^2)}{8\pi}. \quad (5)$$

We can also compute change in pressure due to finite chemical potential as

$$\Delta\mathcal{P}(T, \Lambda, \mu) = \mathcal{P}(T, \Lambda, \mu) - \mathcal{P}(T, \Lambda, \mu = 0). \quad (6)$$

In the left panel of Fig. 4, we plot scaled $\Delta\mathcal{P}$ as a function T for different values of μ/T .

Number Density

Number density is defined as the change of pressure w.r.t. chemical potential; $n(T, \Lambda, \mu) = \frac{\partial\mathcal{P}}{\partial\mu}$. In the right panel of Fig. 4 we plot scaled number density as a function T for different values of μ/T .

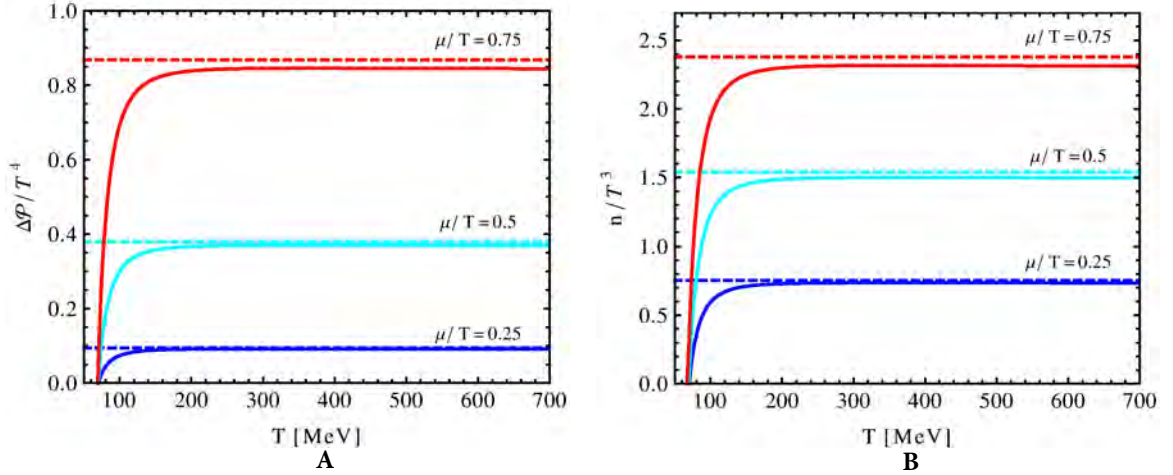


Fig. 4: A: Pressure difference due to finite μ as function of temperature for different values for μ/T with $\Lambda = 2\pi\sqrt{T^2 + \mu^2/\pi^2}$. B: Quark number density for different values for μ/T .

Conclusion

In this article, we have presented the results of a NNLO (three-loop) HTLpt calculation of the thermodynamic potential of QCD at finite temperature and chemical potential(s). Our final result is completely analytic, gauge invariant, and should be valid in the region of the phase diagram for which $\mu \lesssim 2\pi T$. Based on the resulting thermodynamic potential we have calculated the pressure, change in pressure due to chemical potential and number density of the QGP. We have compared our result for pressure with recent lattice data and we found very good agreement down to temperature as low as 200 MeV.

References

1. Andersen JO, Braaten E and Strickland M (2000) Hard thermal loop resummation of the free energy of a hot quark-gluon plasma, *Phys Rev* **D61** 074016

2. Andersen JO, Petitgirard E and Strickland M (2002) Two loop HTL thermodynamics with quarks, *Phys Rev* **D70** 045001
3. Andersen JO, Strickland M and Su N (2009) Three-loop HTL Free Energy for QED, *Phys Rev* **D80**, 085015
4. Andersen JO, Strickland M and Su N (2010) Three-loop HTL gluon thermodynamics at intermediate coupling, *JHEP* **1008**, 113
5. Andersen JO, Leganger LE, Strickland M and Su N (2011) Three-loop HTL QCD thermodynamics *JHEP* **1108** 053
6. Bazavov A *et al.*, (2009) Equation of state and QCD transition at finite temperature, *Phys Rev* **D80** 014504
7. Bazavov A *et al.*, (HotQCD collaboration)(2012) Fluctuations and Correlations of net baryon number, electric charge, and strangeness: A comparison of lattice QCD results with the hadron resonance gas model, *Phys Rev* **D86** 034509
8. Bazavov A *et al.*, (2013) Quark number susceptibilities at high temperatures, *Phys Rev* **88** 094021
9. Bernard C *et al.*, (MILC Collaboration) (2005) QCD thermodynamics with three flavors of improved staggered quarks, *Phys Rev* **D71** 034504
10. Borsanyi S *et al.*, (2010) The QCD equation of state with dynamical quarks, *JHEP* **1011** 077
11. Borsanyi S *et al.*, (2012a) Fluctuations of conserved charges at finite temperature from lattice QCD, *JHEP* **1201** 138
12. Borsanyi S, Durr S, Fodor Z, Hoelbling C *et al.* (2012b) QCD thermodynamics with continuum extrapolated Wilson fermions I, *JHEP* **1208** 126
13. Borsanyi S *et al.*, (2012c) QCD equation of state at nonzero chemical potential: continuum results with physical quark masses at order μ^2 , *JHEP* **08** 053
14. Borsanyi S (2013) Thermodynamics of the QCD transition from lattice, *Nucl Phys* **A904-905** 270c
15. Braaten E and Pisarski RD (1990) Soft Amplitudes in Hot Gauge Theories: A General Analysis, *Nucl Phys* **B337** 569
16. Chakraborty P, Mustafa MG and MH Thoma (2002) Quark number susceptibility in hard thermal loop approximation, *Eur Phys J* **C23** 591
17. Chakraborty P, Mustafa MG and MH Thoma (2003) Quark number susceptibility, thermodynamic sum rule and hard thermal loop approximation, *Phys Rev* **D68** 085012
18. Haque N *et al.*, (2014a) Three-loop HTLpt Pressure and Susceptibilities at Finite Temperature and Density, *Phys Rev* **D89** 061701(R)
19. Haque N *et al.*, (2014b) Three-loop HTLpt thermodynamics at finite temperature and chemical potential, *JHEP* **1405** 027
20. Haque N and Mustafa MG (2010) A Modified Hard Thermal Loop Perturbation Theory, arXiv:1007.2076.
21. Haque N and Mustafa MG (2011b) Quark Number Susceptibility and Thermodynamics in HTL approximation, *Nucl Phys* **A862-863** 271
22. Haque N, Mustafa MG and Strickland M (2013a) Two-loop HTL pressure at finite temperature and chemical potential, *Phys Rev* **D87** 105007

-
23. Haque N, Mustafa MG and Strickland M (2013b) Quark Number Susceptibilities from Two-Loop Hard Thermal Loop Perturbation Theory, *JHEP* **1307** 184
 24. Haque N, Mustafa MG and Thoma MH (2011a) Conserved Density Fluctuation and Temporal Correlation Function in HTL Perturbation Theory, *Phys Rev* **D84** 054009
 25. Petreczky P (2012) Lattice QCD at non-zero temperature, *J Phys* **G39** 093002
 26. Su N, Andersen JO and Strickland M (2010) Gluon Thermodynamics at Intermediate Coupling, *Phys Rev Lett* **104** 122003.